Journal of Optoelectronics and Advanced Materials Vol. 7, No. 4, August 2005, p. 1983 - 1992

STRUCTURAL PROPERTIES OF LIQUID K-Te ALLOYS

G. Tezgor [b], S. S. Dalgic [a, b,*], U. Domekeli [b]

[a] International Center for Physics and Applied Mathematics, Trakya University, P.K. 126, Karaagac, Edirne-Turkey
[b] Department of Physics, Trakya University, 22030 Edirne-Turkey

The structure of K-Te liquid alloys at two different stoichiometric compositions was determined using the effective pair potentials based on the modified analytic embedded atom method (MAEAM) with the Variational Modified Hypernetted Chain (VMHNC) liquid state theory. The MAEAM potential functions are fitted to both solid and liquid state properties for only pure liquid metals. A new effective pair potential form based on the MAEAM has been proposed for the best possible structural properties of these alloys. The partial pair correlation functions for the $K_{0.12}Te_{0.88}$ at T = 723 K and equiatomic KTe at 770 K have been obtained. The results are in reasonably good agreement with experiments and MD results.

(Received May 27, 2005; accepted July 21, 2005)

Keywords: Modified analytic EAM potentials, Structure

1. Introduction

The interatomic potentials for the metallic systems play an important role in the atomic computer simulations, as the accuracy of the potentials will obviously affect the result of the computer simulations. Nowadays, computer simulations have become the increasingly useful tool for studying the structure and properties of metals and alloys. The embedded-atom method (EAM) potentials which was originally proposed by Daw and Baskes (DB) [1] and has been widely used in a wide range of metallic systems in many aspects of computer simulations, such as point defects alloying, segregation, surface, grain boundary structure and so on [2,3]. Based on Daw and Baskes' EAM model, Johnson had presented analytic EAM (AEAM) nearest-neighbor models for b.c.c, f.c.c, and h.c.p. metals and alloys [2,4]. Zhang et al. [5] developed a modified analytic EAM (MAEAM) model based on Johnson's (AEAM) model. Zhang and co-workers calculated the formation enthalpies, point defects, surface structures for disordered solid-solution and ordered inter-metallic compounds and so-on [5-8]. Recently Fang et al. [9] have been constructed the interatomic potentials for binary immiscible alloy systems with MAEAM, and then calculated the formation enthalpies for those systems. They have demonstrated that the MAEAM may be a reasonable method for immiscible alloys by comparing with other potential models [10]. In the literature, there are several versions of EAM which differ by parametrisation methods and functions involved. The parametrisations are performed by fitting the model to bulk solid properties using different energy equations of state. Generally universal equation of Rose et al. [11] is used. Although the EAM primarily developed for the solid phase has also been used in liquid structure calculations with molecular dynamic (MD) simulations or integral equation theories in order to check the accuracy of the forms chosen for the embedding function and pair interaction and of the method used for their parameterisation. In addition, researchers [12-14] found that one of the self consistent integral equation theory, the variational modified hypernetted chain (VMHNC) approximation [15-17] successfully applied to metallic systems in the EAM calculations. It is for this reason that we choose the VMHNC theory for our liquid structure calculations using the MAEAM derived effective pair potentials.

On the other hand, chalcogen liquids in the liquid metals and alloys, such as selenium and tellurium have received considerable attention. It is known that the liquid Te has metallic properties,

* Corresponding author: serapd@trakya.edu.tr, dserap@yahoo.com

while the solid Te is a typical semiconductor. It is noticed that alkali-chalcogen alloy systems exhibit interesting chemical and physical properties due to the large difference in electronegativity of components. Among them the K-Te system shows one of the most complex phase diagram for a binary system. Thermodynamic and electronic properties indicate a similar complex behaviour in the liquid system. Both experimental investigations of the thermodynamic properties and diffraction experiments on K-Te alloys demonstrate that the compound forming tendency has been extended to the liquid state. Neutron diffraction experiments of the equiatomic melt of K-Te alloys have been performed by Fortner and co-workers [18]. The generalized gradient approximation (GGA), has been employed by Hafner and co-workers [19, 20] in the first principal molecular dynamic (FPMD) calculations for $K_{0.67}Te_{0.33}$, $K_{0.50}Te_{0.50}$ and $K_{0.12}Te_{0.88}$ alloys.

According to our knowledge, up to now no MAEAM potential model has been applied to the alkali – tellurium alloy systems. In this work we have studied with recently proposed MAEAM models in order to produce an effective pair potential which is capable of predicting the structural properties of liquid K and Te metals. The parameters of the MAEAM potential functions are parameterized which give a good description of the liquid and still describe the solid accurately. We have improved the functional forms of the effective potentials based on the MAEAM. In order to construct the alloy effective pair potential, two different alloy potential forms has been proposed. One of the purpose of the present paper is to obtain the suitable effective interatomic pair potentials for binary liquid K-Te alloys based on the MAEAM. The presently obtained effective potentials for $K_{0.50}Te_{0.50}$ and $K_{0.12}Te_{0.88}$.alloys are used as input data in the VMHNC [21, 22] structural calculations. We have found that the Finnis-Sinclair [23] type alloy effective potentials reproduce well the observed total structure data for the presented composition of K-Te alloys.

2. Theory

In the MAEAM model, a modified energy term M(P) is added to the total energy expression for the EAM to express the difference between the actual total energy of a system of atoms and that calculated from the original EAM using a linear superposition of spherically averaged atomic electron densities [24]. The total internal energy of system for the MAEAM potentials is written as [25]:

$$E_{tot} = \sum F(\rho_i) + \frac{1}{2}\sum \phi(r_{ij}) + \sum M(P_i), \tag{1}$$

where $F(\rho_i)$ is the embedding function, $\phi(r_{ij})$ is the pair potential between atoms i and j with separation distance r_{ij} and ρ_i is the electron density induced at site i by all other atoms in the system and i is taken in the original form [26]:

$$\rho_i = \sum f(r_{ij}) \tag{2}$$

$M(P_i)$ is the energy modification term which is empirically taken as

$$M(P) = \alpha\left\{1 - \exp\left[-\left(\ln\left|\frac{P}{P_e}\right|\right)^2\right]\right\}. \tag{3}$$

The embedding function $F(\rho)$ and atomic density f(r) are taken the forms as those used by Johnson [27]

$$F(\rho) = -F_0\left[1 - n\ln\left(\frac{\rho}{\rho_e}\right)\right]\left(\frac{\rho}{\rho_e}\right)^n, \tag{4}$$

$$f(r) = f_e \left(\frac{r_{1e}}{r} \right)^6 , \tag{5}$$

where subscript e indicates equilibrium state , r_{1e} is the nearest neighbor distance in equilibrium, $F_o=E_c - E_{1f}$, f_e is taken as $f_e = \sqrt{E_c}/\Omega$ where Ω is the atomic volume. In this work, we assume that metal A and B are b.c.c. and h.c.p. metals, respectively. The energy modification term P in h.c.p metal has the same expression as those for b.c.c metal given in [28] as

$$P_i = \sum_j f^2(r_{ij}) \tag{6}$$

The sum in Eq.(6) is taken to r_c which is defined as the cut-off distance. If the distance between the considered atom and its surrounding atom is smaller than or equal to r_c , the pair potentials are taken as the following equations [9]. For h.c.p metals, it takes

$$\phi(r) = k_0 + k_{-1}\left(\frac{r}{r_{1e}}\right)^{-1} + k_1\left(\frac{r}{r_{1e}}\right) + k_2\left(\frac{r}{r_{1e}}\right)^2 + k_3\left(\frac{r}{r_{1e}}\right)^3 + k_4\left(\frac{r}{r_{1e}}\right)^4 + k_5\left(\frac{r}{r_{1e}}\right)^5 + k_6\left(\frac{r}{r_{1e}}\right)^6 . \tag{7}$$

For b.c.c metals, it is given by

$$\phi(r) = k_0 + k_{-1}\left(\frac{r}{r_{1e}}\right)^{-1} + k_1\left(\frac{r}{r_{1e}}\right) + k_2\left(\frac{r}{r_{1e}}\right)^2 + k_3\left(\frac{r}{r_{1e}}\right)^3 + k_4\left(\frac{r}{r_{1e}}\right)^4 . \tag{8}$$

In the above equations, the fitting parameters for h.c.p. are 10 and for b.c.c. metals are 8. In this work, we concentrate on the liquid state calculations. We have parameterized the potential functions which give a good description of the liquid state properties and still describe the solid state accurately. We assume that if the distance is larger than or equal to r_c, the functions $\phi(r)$, $f(r)$ and their slope go to zero. This is known as two cut off condition:

$$\phi(r_c) = 0 , \qquad f(r_c) = 0 \tag{9– a}$$

$$\phi'(r_c) = 0 , \qquad f'(r_c) = 0 \tag{9– b}$$

The vacancy formation energy E_{1f} is the energy difference between a crystal with one vacancy lattice site and a perfect crystal containing the same number of atoms. In this formalism, this unrelaxed vacancy formation energy can be approximately represented with the pair potential approximation for fitting purposes [2], i.e.

$$E_{1f} = -\frac{1}{2}\sum \phi(r_c) . \tag{10}$$

In the above equations the coefficients α and n can be determined from the following equations.

$$F(\rho_c) = E_{EOS}(a^*) - \frac{1}{2}\sum \phi(r_c) - M(P). \tag{11}$$

where $E_{EOS}(a^*)$ is Rose's equation of state (EOS) for the cohesive energy at given temperature for liquid metals [11]. We have noted that this scheme gives the perfect agreement with experimental values of lattice constant a, cohesive energy E_c and Bulk modulus *B* in their solid state.

In order to obtain the effective pair interactions from the MAEAM, we have extended the Finnis-Sinclair (FS) effective pair potential approximation which is based on the original EAM and used in our previous calculations [29]. We assume that the second and higher derivatives of the

embedding function F are ignored. Thus the atoms interact with the effective pairwise interaction $\phi_{\text{eff}}(\text{r})$ in pure metals given by

$$\phi_{eff}(r) = \phi(r) - 2F'(\rho) f(r) M(P) \tag{12}$$

where $\text{F}'(\rho)$ denotes the first derivative of embedding function. In the present paper, We propose a new alloy effective pairwise potential form based on the FS model as:

$$\phi_{\text{eff}}^{\text{AB}}(\text{r}) = \phi_{\text{AB}}(\text{r}) - 2\text{F}'_{\text{AB}}(\rho)\text{f}_{\text{AB}}(\text{r})\text{M}_{\text{AB}}(\text{P}_{\text{AB}}). \tag{13}$$

where the alloy pair potential $\phi^{\text{AB}}(\text{r})$ between different atomic species is taken as Johnson's formula [2]:

$$\phi^{\text{AB}}(\text{r}) = \frac{1}{2}\left[\frac{\text{f}^{\text{B}}(\text{r})}{\text{f}^{\text{A}}(\text{r})}\phi^{\text{AA}}(\text{r}) + \frac{\text{f}^{\text{A}}(\text{r})}{\text{f}^{\text{B}}(\text{r})}\phi^{\text{BB}}(\text{r})\right] \tag{14}$$

Here AA and BB indicate A and B, type atoms in a binary alloy respectively. $\phi^{\text{AA}}(\text{r})$ and $\phi^{\text{BB}}(\text{r})$ are the monatomic potentials given by Eqs. (7-8) respectively. In the above equations

$$\text{f}_{\text{AB}}(\text{r}) = \text{f}_{\text{eAB}}\left(\frac{\text{r}_{\text{1e AB}}}{\text{r}}\right)^{6} \tag{15}$$

where $\text{r}_{\text{1eAB}} = (\text{r}_{\text{1eAA}} + \text{r}_{\text{1eBB}})/2$, $\text{f}_{\text{eAB}} = (\text{f}_{\text{eAA}} + \text{f}_{\text{eBB}})/2$,

$$\text{M}_{\text{AB}}(\text{P}_{\text{AB}}) = \alpha_{\text{AB}}\left\{1 - \exp\left[-\left(\ln\left|\frac{\text{P}_{\text{AB}}}{\text{P}_{\text{eAB}}}\right|\right)^{2}\right]\right\} \tag{16}$$

where $\alpha_{\text{AB}} = (\alpha_{\text{AA}} + \alpha_{\text{BB}})/2$, $\text{P}_{\text{eAB}} = (\text{P}_{\text{eAA}} + \text{P}_{\text{eBB}})/2$,

$$\text{P}_{\text{AB}} = \sum_{\text{j}} \text{f}_{\text{AB}}^{2}(\text{r}_{\text{ij}}). \tag{17}$$

We have also checked the alternative two-body potential functions of alloy as given below.

$$\phi_{\text{eff}}^{\text{AB}}(\text{r}) = \frac{1}{2}\left[\frac{\text{f}^{\text{B}}(\text{r})}{\text{f}^{\text{A}}(\text{r})}\phi_{\text{eff}}^{\text{AA}}(\text{r}) + \frac{\text{f}^{\text{A}}(\text{r})}{\text{f}^{\text{B}}(\text{r})}\phi_{\text{eff}}^{\text{BB}}(\text{r})\right] \tag{18}$$

$$\phi_{eff}^{AB}(r) = \phi^{AB}(r) \tag{19}$$

The potential form given in Eq. (18) is similar to the modified Johnson potential proposed by Zang et al [25].

3. Liquid state theory

With the effective pair potential known, integral equations are able to provide us the liquid structure for metals. In our structural calculations, one of the integral equation theory which has shown to be very reliable theory of liquids is VMHNC has been carried out [21, 22, 30]. The starting

point of most of the integral equation theories of liquids is the Ornstein-Zernike (OZ) equation, which for a homogeneous, isotropic, binary system reads (i, j =1, 2) can be written as

$$h_{ij}(r) = c_{ij}(r) + \sum_{l=1}^{2} \rho_l h_{il}(r) * c_{lj}(r) \tag{20}$$

which defines the partial direct correlation functions, $c_{ij}(r)$, in terms of the total correlation functions, $h_{ij}(r) = g_{ij}(r) - 1$ where $g_{ij}(r)$ denote the partial pair distribution functions and ρ_l denote the partial ionic number densities. Eq.(20) is supplemented by the exact closure relation

$$c_{ij}(r) = h_{ij}(r) - \ln\left[g_{ij}(r) e^{\beta\phi_{ij}(r) + B_{ij}(r)}\right] \tag{21}$$

where $\phi_{ij}(r)$ are the interatomic pair potentials and the $B_{ij}(r)$ denotes the PY bridge functions for binary system. For binary fluids, we have now a set of three coupled integral equations relating the $g_{ij}(r)$ to $\phi_{ij}(r)$. We have carried out the VMHNC integral equation theory in which was extended by Gonzalez *et al*. [21], so as to minimize the configurational Helmholtz free energy functional $f^{VMHNC}(\beta, \rho, x_l, \eta_\alpha)$ by the variational condition for the m component system.

$$\frac{\partial f^{VMHNC}(\beta, \rho, x_1, \eta)}{\partial \eta_k} = 0, \qquad k=1,2....,m \tag{22}$$

The total structure factors for liquid alloys are determined as a linear combination of partial structure factors [31] given by

$$S(q) = \sum_{i,j} b_i b_j S_{ij}(q) / < b >^2 \tag{23}$$

$$< b >^2 = \left(\sum_i b_i \right)^2, \tag{24}$$

where b_i and b_j are the neutron scattering amplitudes which are taken from [20].

4. Results and discussion

4.1 Simple metals

The input parameters, such as the ionic number densities and thermodynamic states for liquids K and Te are taken from Waseda [32] and given in Table 1 where s and *l* indicate the solid and liquid phases, respectively. E_c^s and a^s values are taken from Kittel [33] In this work for the purpose of the liquid state calculations, we have used the Rose's equation of state (EOS) [11] to calculate the cohesive energy for pure metals at given temperature. We have determined the parameters of the potential functions by combining the two equations for the cut off procedure (Eqs. 9) and the equation of the equilibrium condition (Eq. 10), the equation for the cohesive energy (Eq. 11) and the equation for minimizing the configurational free energy (Eq. 22). We must say that we have not fitted the Helmholtz free energy. Following others, the set of parameters have been chosen to give the best possible values for the liquid structure. The optimized potential parameters for K and Te which have been obtained at near their melting are presented in Table 2. We note here that the r_c values listed in table 2 are different from those of FPMD calculations because the value of r_c are always larger than in solids.

Table 1. The input data used in our calculations. ρ number density (atoms/Å^3), a lattice constant (Å) , E_c cohesive energy in eV.

	T (K)	ρ (atoms/ Å^3)	a^s (Å)	a^l (Å)	E_c^s (eV)	E_c^l (eV)
K	723	0.0114	5.225	5.598	0.934	0.926
Te	743	0.0273	3.883	3.991	2.19	2.187

Table 2. The MAEAM potential parameters for K and Te.

Te		K	
Parameter	Value	Parameter	Value
n	0.8300	n	0.4516
$F_0(eV)$	1.45862	$F_0(eV)$	0.61749
α (eV)	0.040038	α (eV)	0.31746
$K_{-1}(eV)$	42.60208	$K_{-1}(eV)$	37.22396
$K_0(eV)$	-187.38786	$K_0(eV)$	-159.58595
$K_1(eV)$	349.04768	$K_1(eV)$	275.73292
$K_2(eV)$	-359.11337	$K_2(eV)$	-240.06857
$K_3(eV)$	221.12729	$K_3(eV)$	105.10185
$K_4(eV)$	-81.61164	$K_4(eV)$	-18.45449
$K_5(eV)$	16.72094	r_c(Å)	6.45
$K_6(eV)$	-1.46654		
r_c(Å)	5.12		

Fig. 1 shows the MAEAM embedding energy functions for liquids K and Te. The difference in both the depth and position of the embedding function indicates the large difference in electronegativity of tellurium and potassium.

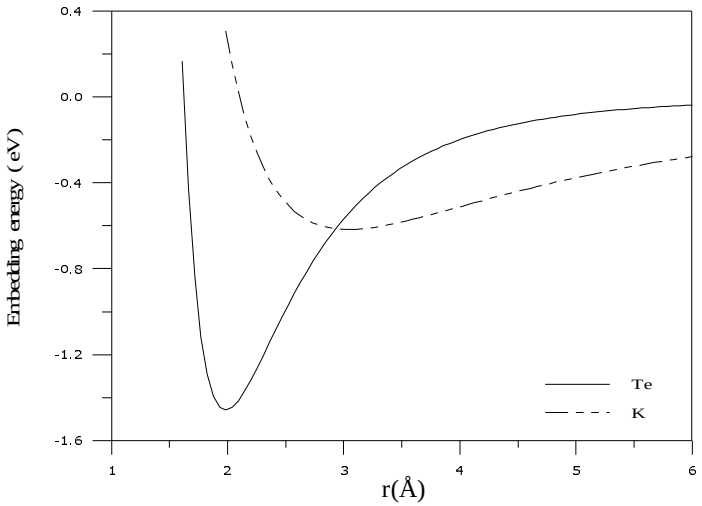

Fig. 1. MAEAM embedding energy function for liquids Te and K.

The constructed MAEAM effective pair potentials for K and Te are used as input data in our structural calculations using the VMHNC approximation. Fig. 2 shows the calculated pair distribution functions for liquids K and Te compared to the experimental data of Waseda [32]. For comparison the experimental results of Shimojo [34] are illustrated for Te.

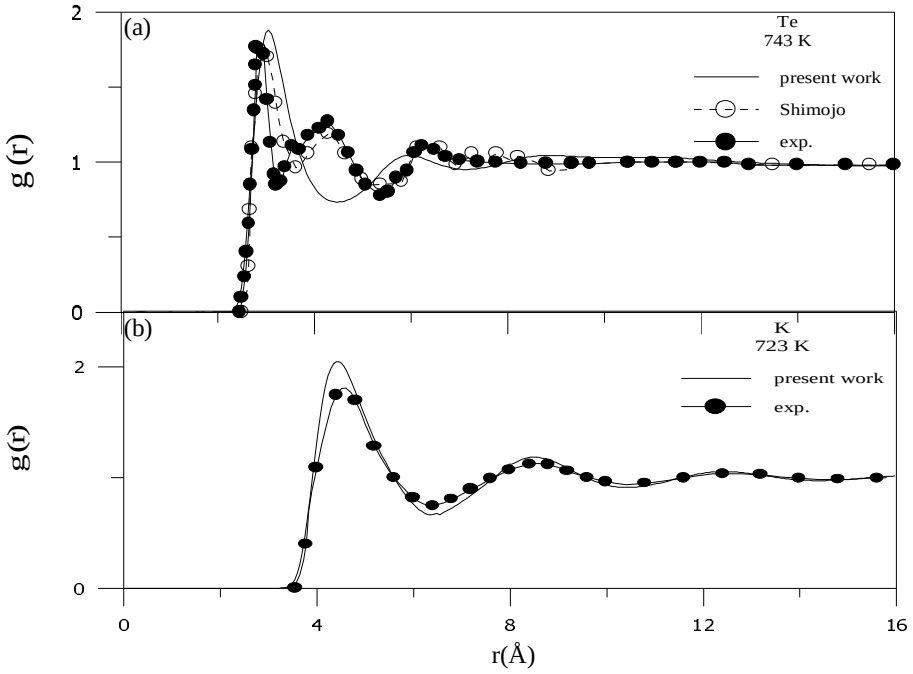

Fig. 2. Pair distribution functions for (a) liquid Te and (b) liquid K. The experimental data are taken from Waseda [32].

The agreement between the calculated VMHNC results using the effective potential presently determined and the experimental data is a good for liquid K. For liquid Te, the double peak is observed in both the experimental data. The VMHNC result for liquid Te clearly differs from the experimental data in the first neighbor region of the pair distribution function. However the medium, long range r region and the pair distribution is well reproduced.

4.2 The K-Te alloys

As described in the preceding section, we have extended the Fang' MAEAM to study the structural properties of the liquid binary K-Te alloys. The resultant FS type alloy effective potentials are shown in Fig. 3a. The different forms of alloy potentials are compared with each other in Fig.3b. As seen Fig. 3a that these partial pair potentials give the correct trends as far as the position of the concerned. As we go from K to Te in periodic table, the calculated potentials becomes flatter and the width increases. In Fig. 3b, the FS type alloy potential is deeper than the Johnson and modified Johnson potentials. But when r is larger than r_{1e}, the present potential coincides with others. We note that there is not a clear difference in the structural calculations using these potentials. These effective pair potentials are used the input data in our structural calculations. In. Fig. 4, we have presented the calculated VMHNC partial distribution functions for Te-Te and K-Te in $K_{0.12} - Te_{0.88}$ composition by comparing with those obtained by Kresse – Hafner [20].

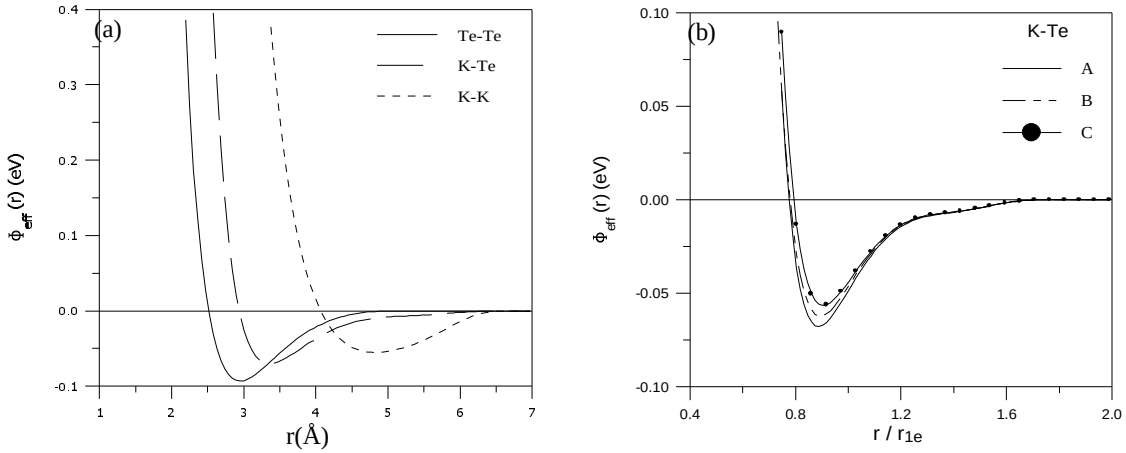

Fig. 3. (a) MAEAM effective pair potentials for $K_{0.12}$-$Te_{0.88}$ alloy. (b) Comparison of the alloy effective potentials those obtained by different forms: (A) FS type MAEAM (B) Modified Johnson [25] (C) Johnson potentials [2].

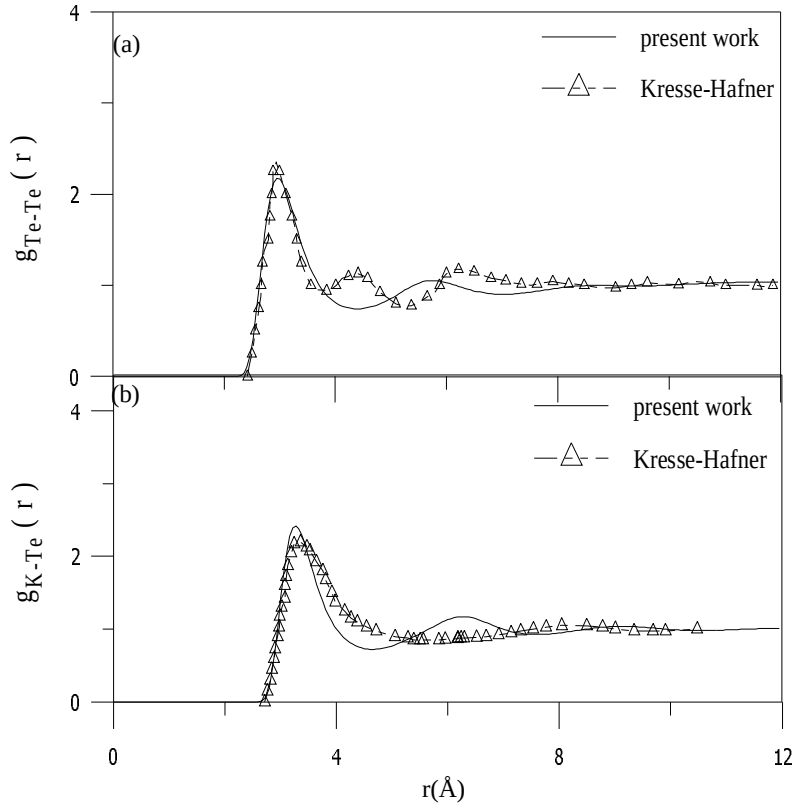

Fig. 4. Partial pair distribution functions for (a) $g_{Te-Te}(r)$ (b) $g_{K-Te}(r)$ in $K_{0.12}Te_{0.88}$ at 723 K.

It is seen in Fig. 4 that the present results correctly predict the position and height of the first peak of experimental pair distribution function. We note that with decreasing temperature the height of the main peak of $g_{Te-Te}(r)$ increases. When the K concentration is increased, the first minimum of the $g_{Te-Te}(r)$ becomes deeper and the first peaks of the $g_{K-Te}(r)$ become larger. Kresse –Hafner [20] found that the structure of the $K_{0.50}$-$Te_{0.50}$ is in good agreement with experiment. The calculated

total structure factors S(Q) for each alloy composition studied in this work are illustrated in Fig. 5 and Fig. 6, respectively. We can not able to compare our results for total S(Q) with those obtained by Kresse-Hafner. Fig. 5 shows that the height of the calculated total structure factor is overestimated compared to experiment for $K_{0.12}$ – $Te_{0.88}$ composition. Also there are small differences in the phase of oscillations. For the equaltomic alloy composition of K-Te alloy, it is clear that the position of the main peak is well predicted using the effective pair potentials based on MAEAM.

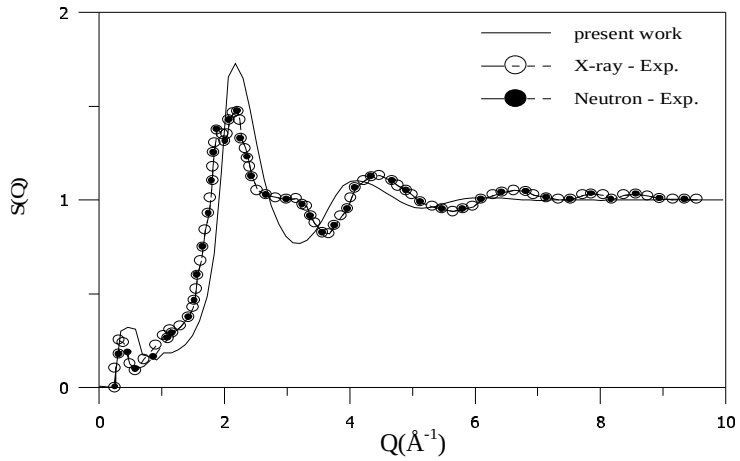

Fig.5. Total Static structure factors: $K_{0.12}$-$Te_{0.88}$ at 723 K

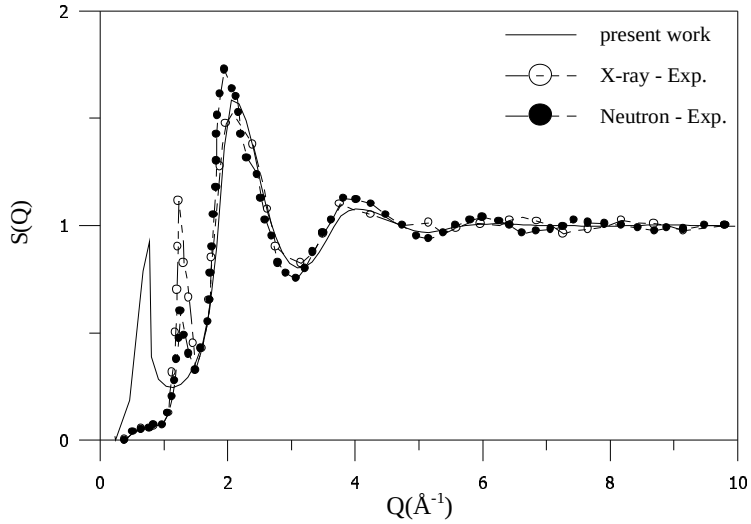

Fig. 6. Total static structure factors: $K_{0.50}$-$Te_{0.50}$ at 770 K.

In Fig. 6, the calculated structure factors also reproduce the pre-peak at about Q = 0.5 $Å^{-1}$. This may be attributed to long-range behaviour of the potential. It appears that the MEAM potentials predict the total structure factors in better accord with the experimental trends. The overall agreement with experiment is a high degree for the equi-atomic composition of K-Te alloy.

5. Conclusions

The presented MAEAM provides a realistic description of the pair interaction in liquid K-Te alloys. These calculations were performed with the potential functions that not only fit to solid data

but also liquid state properties. Since the embedding function and pair potential in the pure liquid metals are different from those of the solid, we have improved the functional forms of the effective pair potentials to obtain a good description of the liquid and still describe the solid accurately. We note that our effective pair potentials show long-range character different from other MAEAM derived potentials for solids. The structural calculations were carried out using MAEAM derived effective pair potentials with the VMHNC theory of liquids. Comparison between the results of the VMHNC theory and available experimental data show that the proposed MAEAM formalism for K-Te alloy systems is capable of providing a good description in their liquid state. Our results suggest that the effective alloy pair potential based on the MAEAM model is a very good approximation for the study of liquid alkali- tellurium alloys. The discrepancies with experiment make further investigations necessary. The constructed MAEAM potentials can be used in further modelling of thermodynamic and other properties of K-Te alloys with molecular dynamic and Monte Carlo simulations.

References

[1] M. S. Daw, M. I. Baskes, Phys. Rev. Lett. **50**, 1285 (1983).
[2] R. A. Johnson, D. J. Oh, J. Mater. Res. **4**, 1195 (1989).
[3] T. P. Swiler, R. E. Loehman, Acta Mater. **48**, 4419 (2000).
[4] R. A. Jonhson, J. Mater. Res. **3**, 471 (1988).
[5] B. W. Zhang, Y. F. Ouyang, Phys. Rev. **B 48**, 3022 (1993).
[6] B. W. Zhang, Y. F. Ouyang, S. Z. Liao, Z. P. Jin, Physica **B 262**, 218(1999).
[7] W. Y. Hu, B. W. Zhang, B. Y. Huang, F. Gao, D. J. Bacon, J. Phys. Condens. Matter **13**, 1193 (2001).
[8] B. W. Zhang, Y. F. Ouyang, S. Z. Liao, Z. P. Jin, Trans. Nonferrous Met. Soc. China **6**, 52 (1996).
[9] F. Fang, X. L. Shu, H. Q. Deng, W. Y. Hu, M. Zhu, Mater. Sci. and Eng. **A**, 355 357-367 (2003).
[10] Y. F. Ouyang, B. W. Zhang, S. Z. Liao, Z. P. Jin, Z. Phys. **B 10**1, 161 (1996).
[11] J. H. Rose, J. R. Smith, F. Guinea, J. Ferrante, Phys. Rev. **B 29**, 2963 (1984).
[12] G. M. Bhuiyan, M. Silbert, M. J. Stott, Phys. Rev. **B 53**, 636 (1995).
[13] G. M. Bhuiyan, M. A. Khaleque, J. Non – Cryst. Solids, **226**, 175 (1998).
[14] M. M. G. Alemany, C. Rey, L. J. Gallego, Phys. Rev. **B 58**, 685 (1998).
[15] Y. Rosenfeld, J. Stat. Phys. **42**, 437 (1986).
[16] L. E. Gonzalez, D. J. Gonzalez, M. Silbert, Phys. Rev. **A 45**, 3803 (1992); L. E. Gonzalez, M. Silbert, D. J. Gonzalez, S. Dalgıç, Z. Phys. **B103**, 13 (1997).
[17] S. S. Dalgic, S. Dalgic, S. Sengul, M. Celtek, G. Tezgor, J. Optoelectron. Adv. Mater. **3**, (4) 831 (2001).
[18] J. Fortner, M.-L, Saboungi, J. Enderby, Phys. Rev. Lett. **69**, 1415 (1992).
[19] K. Seifert-Lorenz, G. Kresse, J. Hafner, J. Non-Cryst Solids **293-295**, 193-198 (2001).
[20] K. Seifert-Lorenz, G. Kresse, J. Hafner, J. Non-Cryst Solids **312-314**, 371-375 (2002).
[21] L. E. Gonzales, A. Meyer, M. P. Iniguez, D. J. Gonzales, M. Silbert, Phys. Rev **E47**, 4120 (1993).
[22] H. Kes, S. S. Dalgıc, S. Dalgıc, G. Tezgor, J. Optoelectron. Adv. Mater. **5**, 1281 (2003).
[23] M. W. Finnis, J. E. Sinclair, Phil. Mag. **A 50**, 45 (1984).
[24] H. Q. Deng, W. Y. Hu, X. L. Shu, L. Zhang, B. W. Zhang, Surf. Sci. **517**, 177 (2002).
[25] B. W. Zhang, Y. F. Ouyang, Phys. Rev. **B 48**, 3022 (1993).
[26] R. A. Johnson, Phys. Rev. **B 37**, 3924 (1988).
[27] R. A. Jonhson, Phys. Rev. **B 39**, 12554 (1989).
[28] B. W. Zhang, Y. F. Ouyang, S. Z. Liao, Z. P. Jin, Physica **B 262**, 218 (1999).
[29] S. S. Dalgic, S. Dalgic, U. Domekeli, J. Optoelectron. Adv. Mater. **5**, 1263 (2003).
[30] S. S. Dalgıc, S. Dalgıc, G. Tezgor, Phys. And Chem. Liq. **40**, 539 (2002).
[31] V. M. Glazov, L. M. Pavlova, Scandinavian J. of Metallurgy **31**, 52-58 (2002).
[32] Y. Waseda, The Structure of Non – Crystalline Materials, McGraw – Hill, New York (1981).
[33] C. Kittel, Introduction to Solid State Physics, 6 th edition (1986).
[34] F. Shimojo, K. Hoshino, Y Zempo, J. Non-Cryst Solids **250-252**, 547 (1999).